JPMTR 053 | 1413
DOI 10.14622/JPMTR-1413
UDC 6551 : 532.6-035

Research paper
Received: 2014-07-15
Accepted: 2014-11-28

Inkjet printed hydrophobic microfluidic channelling on porous substrates

Risto Koivunen[1], Eveliina Jutila[1], Patrick Gane[1,2]

[1] School of Chemical Technology,
Department of Forest Products Technology,
Aalto University, PL 16400, 00076 Aalto, Finland

Emails: risto.koivunen@aalto.fi
eveliina.jutila@aalto.fi

[2] Omya International AG, Baslerstrasse 42,
CH-4665 Oftringen, Switzerland

E-mail: patrick.gane@omya.com

Abstract

Paperfluidic devices consist of patterned microfluidic channels formed on paper or paper-like material. The direction of surface and bulk liquid flow is typically controlled by patterning hydrophobic barriers on the otherwise hydrophilic paper substrate. A variety of hydrophobic materials and functional printing methods can be used for the patterning. Unlike conventional graphical printing, hydrophobising ink must penetrate the whole depth of the substrate to form an effective barrier against leakage from the channel. This study focuses on the development of solvent-based hydrophobic inks for inkjet printing of microfluidic patterning. Hydrophobic inks were produced by dissolving alkyl ketene dimer (AKD) and polystyrene (PS) in p-xylene. Hydrophobic test patterns were inkjet printed with these inks on two highly porous filter papers. The AKD-based ink was found to produce effective hydrophobic barriers but suffered from poorly defined borders. The PS-based ink produced well defined borders, but could only penetrate the full depth of the substrate on one of the chosen papers. Adding PS to AKD ink improved jettability. Hydrophobic ink penetration into filter paper was found to take place as surface film flow over the skeletal fibre structure of the paper. Therefore, paper fibre surface properties and ink surface tension and viscosity are considered to play controlling roles in determining the penetration depth. Differences seen with respect to aqueous wicking behaviour at the interface/border between hydrophilic and hydrophobic regions might be due to the Marangoni derived coffee stain effect and likely to interactions with the fibre surfaces.

Keywords: functional printing, hydrophobic ink, polystyrene, alkyl ketene dimer, paperfluidics

1. Introduction and background

Paperfluidic devices are being developed as a low cost application for functional microfluidics in the field of lab-on-a-chip devices, intended to provide simple, transportable, disposable and self-sufficient analytical tools for a variety of applications including medical diagnostics and environmental monitoring. On such devices, designed for aqueous liquids, samples flow along hydrophilic channels through or to assay zones, where they chemically interact with pre-applied reagents. Results of such reactions can then be analysed visually based on colour, or by external instrumentation, to obtain information on the contents of the test samples (Ballerini, Li and Shen, 2012; Liana et al., 2012).

Based on their design, paperfluidic devices can be divided into three categories of dimensional constructions, i.e., 1D, 2D and 3D devices. In 1D devices, such as commercially available early pregnancy tests, liquid is carried only in a single direction (Dharmaraja et al., 2013). In 2D devices, first introduced in 2007, aqueous liquid flows along channels created by patterning hydrophobic barriers onto an otherwise hydrophilic base substrate (Martinez et al., 2007). This provides room for more complicated assays and for multiple assays on a single device. 3D devices are produced by layering multiple 2D devices on top of each other, allowing liquid to flow both within the layers and from one layer to another (Martinez, Phillips and Whitesides, 2008).

A variety of hydrophobic materials and printing methods have been recently demonstrated as feasible ways of producing hydrophobic patterns on highly permeable filter or chromatography papers. The most prevalent of these methods is inkjet printing, demonstrated with hot-melt wax (Carrilho, Martinez and Whitesides, 2009), solvent-diluted polydimethylsiloxane (Määttänen et al., 2011), UV-polymerising materials (Maejima et al., 2013), acrylic polymer in solvent-based solution (Apilux et al., 2013) and paper sizing agents in solvent-based solution (Li, Tian and Shen, 2010) as well as in the form of aqueous emulsions (Wang et al., 2014; Xu and Enomae, 2014). Other printing methods typically demonstrated

include flexographic printing of solvent-based polystyrene ink (Olkkonen, Lehtinen and Erho, 2011) and screen-printing of candle-making wax (Dungchai, Chailapakul and Henry, 2011).

Unlike conventional graphical printing, in patterning paperfluidic devices hydrophobising ink has not only to cover the surface but also penetrate the whole depth of the hydrophilic substrate in order to produce properly functioning barriers without leaks (Ballerini, Li and Shen, 2012). This full depth penetration can be assisted by having ready wetting of the substrate by the ink, low ink viscosity, high substrate permeability or large volume of applied ink. Wax-printed substrates, for example, are heated after printing to melt the wax and make it penetrate into the pores.

This study, based in part on a thesis work (Koivunen, 2014), focuses on the development of simple low cost solvent-based hydrophobic inks for inkjet printing of microfluidic patterning on porous paper substrates. For this purpose, two different hydrophobising agents, polystyrene (PS) and alkyl ketene dimer (AKD – a paper sizing agent), were used to manufacture inks, both on their own and combined. So far, studies published about hydrophobising agents have usually reported results for only a single material in isolation, with only one published study comparing multiple hydrophobising agents, specifically wax, AKD and methylsilsesquioxane (Wang et al., 2014). Also, no known studies to date have combined multiple hydrophobising materials into a single ink.

Various aspects of these inks and their interaction with substrates were studied. Firstly, the physical ink properties and jettability were characterised. Secondly, physical pattern dimensions achievable by different ink, substrate and print setting combinations were studied. Thirdly, functionality and reliability of the printed patterns in directing flow of aqueous liquid were tested.

Jettability of inkjet inks can be characterised by the inverse Ohnesorge number Z (Jang, Kim and Moon, 2009), a dimensionless number defined as

$$Z = \frac{1}{Oh} \qquad [1]$$

where

$$Oh = \frac{\sqrt{We}}{Re} = \frac{\eta}{\sqrt{a \varrho_{\text{ink}} \gamma}} \qquad [2]$$

in which Re stands for the Reynolds number, We the Weber number, a the characteristic dimension over which flow occurs (the nozzle radius), ϱ_{ink} the ink density, γ the ink surface tension and η the ink viscosity. A good jettability range for Newtonian liquids has been proposed to be $4 < Z < 14$ (Jang, Kim and Moon, 2009), with fluids of higher values of Z exhibiting satellite droplet formation, while those with lower values of Z require excessively long periods of time for the connecting filament to break free from the nozzle, or possibly do not jet at all.

Inkjet printing of solvents containing PS in solution has been reported previously (de Gans et al., 2004; Hoath, Hutchings and Martin, 2009), with molecular weight demonstrated to have a significant effect on jettability due to non-Newtonian rheological behaviour of polymer containing solutions in the print head. However, this viscoelastic behaviour has no significant effect on drop impact or spreading, at least in the case of a non-porous substrate (Jung, Hoath and Hutchings, 2013). High molecular weight polymers can also be liable to degradation by central scission in the print head (A-Alamry et al., 2011).

The feasibility of using PS-containing ink for hydrophobic patterning of paper has, to our knowledge, only been studied once in the literature, using flexographic printing as the patterning method (Olkkonen, Lehtinen and Erho, 2011). In that study, printing had to be carried out on both sides of a substrate, since insufficient depth coverage was achieved with single-sided printing. Another known method involving PS is etching of hydrophilic channels with pure solvent using inkjet printing onto a sheet of paper that has been impregnated beforehand with PS (Abe, Suzuki and Citterio, 2008). However, this method requires up to ten sequential printings to re-deposit enough PS from the channels to their edges, making it a rather slow procedure in practice.

AKD, chosen as a reference material in this study, has previously been successfully inkjet printed to produce paperfluidic devices (Li, Tian and Shen, 2010; Wang et al., 2014). Alternatively, AKD impregnated paper has been patterned by using selective plasma treatment to return areas of paper back to the hydrophilic state (Li et al., 2008). AKD is a paper sizing agent that reacts with hydroxyl groups on the cellulose surface, replacing them with hydrophobic β-keto ester groups.

Physical resolution and functional dimensions reported for paperfluidic patterning methods usually include minimum widths for reliably working barriers and channels. Barriers are those hydrophobic structures separating hydrophilic sections, and the minimum width (nominal or measured) indicates the pattern width required to achieve reliable full depth coverage. Channels are hydrophilic areas limited by the barriers, where liquid will flow in a controlled fashion. Minimum channel width indicates the mean channel width where liquid will still flow reliably, and, with channels narrower than this, irregularities in barrier edge definition will start to block the channel.

2. Materials and methods

2.1 Inks

The chosen hydrophobising agents used in this study were 35 kDa molecular weight polystyrene (Sigma-Aldrich, product code 331651) and solid alkyl ketene dimer Basoplast 88 (BASF). These were dissolved in p-xylene solvent (Acros Organics or Fluka) to produce the hydrophobising inks. This solvent has a viscosity of 0.648 mPa s and the surface tension 28.37 mN m^{-1} at 20 °C, making it suitable for the printer used in this study. Furthermore, p-xylene has been previously shown to be a suitable solvent for PS ink printed with flexography (Olkkonen, Lehtinen and Erho, 2011).

Three inks were produced, with the first one containing 5 % by weight PS, the second one containing 6 % by weight AKD and the third one containing 2 % by weight PS and 6 % by weight AKD. These inks will be henceforth referred to as PS, AKD and AKD-PS inks, respectively. During the study, a total of 5 batches of PS ink, 2 batches of AKD ink and 1 batch of AKD-PS ink were produced.

Cyan and magenta dyes in water were used to visualise hydrophilic regions. The cyan dye solution consisted of 0.2 % by weight concentration of nickel(II) phthalocyanine-tetrasulphonic acid tetrasodium salt (Sigma-Aldrich), supplied as dry powder, dissolved in distilled water. The magenta dye solution consisted of 10 % by weight concentration of commercial carmine food colorant (Dr. Oetker), provided as a highly concentrated aqueous solution, diluted accordingly with distilled water.

2.2 Substrates

Two different commercial filter papers, Whatman grades 1 and 4 (GE Healthcare), manufactured from cotton cellulose, were selected as test substrates for printing. Information about technical properties of these substrates, as provided by the manufacturer, is listed in Table 1.

The porosity ε of each substrate was determined by calculation from the thickness dimension of the sheet and the physical parameters of the paper constituents, namely using Equation 3

$$\varepsilon = 1 - \frac{b}{h\varrho_{\text{solid}}} \qquad [3]$$

where b is the basis weight, h the thickness of the sheet and ϱ_{solid} the density of the solid phase. For cellulose, ϱ_{solid} reported in literature is 1 540 kg dm^{-3} (Koivula et al., 2013).

Table 1: Substrate properties

Substrate	Whatman 1	Whatman 4
Thickness (μm)	180	205
Basis weight (g m^{-2})	88	96
Particle retention under filtration (μm)	11	20–25
Air flow permeability (s/100 cm^3/in^2)	10.5	3.7
Porosity (%)	68	70

2.3 Equipment

Ink surface tension was measured with a CAM200 contact angle measurement system (KSV) using the pendant drop method in a laboratory room maintained at 23 °C. Ink viscosity was determined using an MCR-300 rheometer (Paar-Physica) with a PP50 flat disc spindle and a P-PTD 150 Peltier temperature controlled base plate. Viscosity measurements were conducted at a shear rate of 100 s^{-1} and with the Peltier base plate set at 30 °C.

The inks were printed with a Dimatix material printer DMP-2831 (Fujifilm Dimatix), using the manufacturer's DMC-11610 ink cartridges with nominal 10 pl drop volume. Jettability of the inks was studied using the integrated drop watcher camera, observing drop velocity and satellite droplet formation as functions of drive voltage and jetting frequency, which were increased in 1 V and 2 kHz intervals, respectively.

For image analysis, printed samples were scanned with an Epson Expression 1680 scanner (Seiko Epson) and analysed with ImageJ software version 1.44p (National Institute of Health) to calculate the dimensions of printed barriers and channels. The software functionality setting "Analyze particles" was used to measure the area of a scanned section of channel or barrier. The area was then divided by the length of the scanned section to obtain mean width.

2.4 Print settings and post-print treatment

The inks were printed from the print head, set to 30 °C, onto the substrates held by vacuum on the mounting platen, set to 28 °C. The drive waveform "high viscosity short polymer" provided on the Dimatix device was used in all cases, as it was seen to provide the best jetting. Patterns were printed with a variety of drop spacing values, ranging from 10 to 50 μm (equivalent to 2 590 to 518 dpi).

Prints containing only dissolved PS were ready to use immediately after the solvent had evaporated. The AKD containing prints required curing in an oven or on a laboratory hot plate at 100 °C for 10 minutes to ensure that the AKD had reacted properly with the substrate cellulose.

2.5 Test patterns

Due to the recent introduction of 2D paperfluidics, no standard method exists yet for evaluating properties of printed hydrophilic channels and hydrophobic barriers on porous substrates. Therefore, a test method was developed for this study, strongly inspired by prior examples in the literature (Carrilho, Martinez and Whitesides, 2009). For this method, three different test patterns ("lines", "channels" and "barriers") were created, using the pattern editing software provided with the printer, and printed on the test substrates with the designed inks. The printed patterns were effectively invisible when dry, but became visible when wetted, as demonstrated in Figure 1. This is due to an opacity change in hydrophilic regions as pores are filled with water.

Figure 1: Wetting causes a visible opacity change in the hydrophilic areas; displayed here are two Aalto University logotypes printed with PS ink, shown dry (left) and after dipping in water (right)

For testing how the printed patterns affect liquid transport, cyan dyed water was allowed to wick up along the hydrophilic regions from the bottom edge of the printed samples. For this purpose, the test prints were suspended vertically in jars containing dyed water at the bottom, as demonstrated in Figure 2. By using dyed rather than clear water, the results could be more easily observed during testing and also analysed later on when the samples were dry.

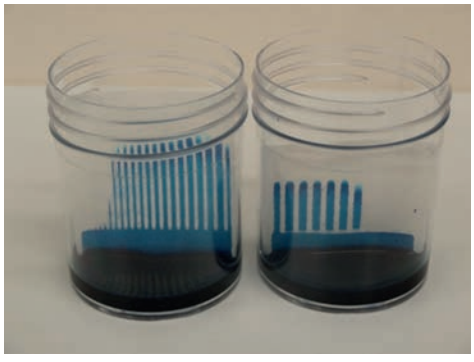

Figure 2: Experimental set-ups for testing channels (left) and barriers (right); cyan coloration indicates areas where water has wicked

The first pattern ("*lines*"), designed to measure line spreading, featured ten 35 mm long straight lines. These varied in nominal width from 0.1 to 1.0 mm in 0.1 mm increments. Cyan dyed water was allowed to wick up the channel until it fully surrounded the top of the lines, after which the samples were dried and scanned to determine actual line widths on the printed and reverse (non-printed) sides.

The second pattern ("*channels*"), designed to measure working channel widths, shown in Figure 3, featured 22 hydrophilic channels 32 mm long and of varying nominal widths, from 0.5 to 2.6 mm in 0.1 mm increments. Cyan dyed water was allowed to wick up the channels for 5 minutes, after which the test samples were dried and scanned to determine actual channel widths. The samples were also examined to determine the narrowest channel where the liquid could travel the full length of the channel within the given time.

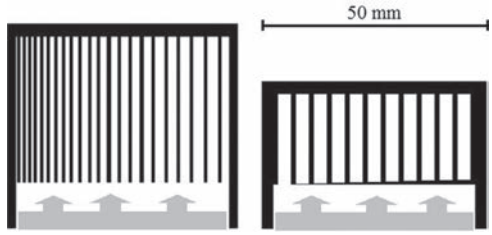

Figure 3: Test patterns for channels (left) and barriers (right); black indicates the hydrophobic region, white the hydrophilic region, with light grey indicating the original exposure to an effectively unlimited source of dyed water as well as the direction of subsequent wicking

The third pattern ("*barriers*"), designed to measure barrier widths required to contain liquid, also shown in Figure 3, featured ten hydrophilic channels with barrier structures of varying widths printed across them, as well as one control channel without any barrier. For samples printed with PS containing ink, the barriers ranged in nominal width from 0.1 to 1.0 mm in 0.1 mm increments. For samples printed with AKD containing inks, nominal barrier widths ranged from 0.05 to 0.50 mm in 0.05 mm increments. Dyed water was allowed to try to wick past the barriers for 30 min, with samples observed every 5 minutes to determine which of the barriers had been penetrated. After this, magenta dyed water was added to the channels that had not been penetrated, followed by drying and scanning of the test devices to determine the actual width of the non-penetrated barriers on the printed side.

Studied sample sizes for given ink/substrate/drop spacing combinations were 5 samples for lines, 10 samples for channels and 10 samples for barriers. For a barrier to be considered reliable, it needed to resist penetration on all 10 tested samples. Similarly, for a channel to be considered reliable, it needed to transport liquid properly on all 10 tested samples.

3. Results

3.1 Ink properties and jettability

The physical properties of the inks, measured from a single batch per ink, are listed in Table 2. Values for Z have been calculated according to Equation 1, with a nozzle radius, a, of 10.5 μm. The reported viscosity values were measured at the relatively low shear rate of 100 s^{-1}, which is not representative of the high shear rates to be found within the print head, but partly reflects the close to static viscoelasticity, i.e., the viscoelasticity existing under small applied strain contributes to the apparent shear viscosity at low shear. All of the inks tested also displayed shear thickening when tested over the shear rate range of 100 to 1 000 s^{-1}, but the available instrumentation, limited to small volumes, did not provide the possibility to test viscous behaviour at shear rates beyond this shear thickening region.

Table 2: Ink properties

Ink	Ink content	Viscosity at 30 °C (mPa s)	Surface tension at 23 °C (mN m^{-1})	Z
PS	PS (5 %)	1.21 ± 0.07	28.18 ± 0.15	13.2
AKD	AKD (6 %)	0.63 ± 0.04	28.54 ± 0.21	25.5
AKD-PS	PS (2 %) and AKD (6 %)	0.90 ± 0.04	28.35 ± 0.12	17.8

Jettability tests showed that the PS ink was jettable up to 10 kHz, though 6 kHz provided more stable performance. The AKD ink was only jettable at 2 kHz, while the AKD-PS ink was jettable up to 6 kHz. At higher frequencies than these, jetting tended to become unstable, easily resulting in nozzle plate flooding. The actual printing frequency was set at 2 kHz for the AKD ink and 6 kHz for the PS and AKD-PS inks.

Drop velocities during jetting have been observed to increase approximately linearly as a function of the jetting voltage (Hoath et al., 2013). In the present study, the PS and AKD-PS inks behaved in this fashion. However, with the AKD ink the velocity peaked at 8 m s^{-1} and could not be increased beyond this level by further increases in jetting voltage. However, this velocity was still within the recommended velocity range of 5–10 m s^{-1} for the printer. Based on drop velocity studies, the drive voltages for the inks for actual printing were set at 18 V for AKD ink, 16 V for AKD-PS ink and 28 V for PS ink, resulting in jetting velocities in the 8–9 m s^{-1} range.

Satellite droplets were observed for all inks under all tested jetting conditions, and could not be fully eliminated in this study. This is not particularly surprising, considering the high values of Z for the inks, resulting from their low viscosities.

3.2 Line spreading

On the printed side, significant line spreading could be observed for all of the inks. On the reverse (non-printed) side, the lines on some samples are slightly narrower than on the printed side, and in some cases they were discontinuous, indicating that the printed ink had achieved full depth coverage only locally. The well-defined and continuous lines tended to have widths of at least 500 μm, with narrower lines displaying discontinuity.

Closer drop spacing, resulting in a higher volume of ink being applied for a given nominal line width, resulted in greater line spreading. Widening the nominal line width resulted in slightly reduced relative line spreading. Some examples of the relative line width for PS and AKD inks as a function of nominal line width are shown in Figure 4.

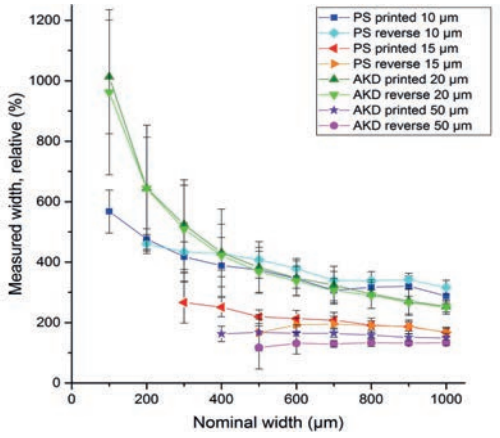

Figure 4: Relative line widths, in terms of nominal width, for Whatman 4 filter paper printed with PS ink at 10 and 15 μm drop spacing, and with AKD ink at 20 and 50 μm drop spacing

The AKD and AKD-PS inks exhibited roughly similar line spreading. The PS ink could not be directly compared with the others, due to PS ink requiring a drop spacing of 15 μm or less for full depth coverage. Trying to print the same test pattern with AKD or AKD-PS inks with such a close drop spacing resulted in some of the lines merging with their neighbours, so that widths of all lines could no longer be measured.

3.3 Hydrophobic barriers

Barrier penetration was observed at 5 min intervals for 30 min. For most of the barriers that were penetrated this happened within the initial 5 minutes, with usually only a small portion of barriers being penetrated after that. An exception to this was PS ink on Whatman 1, where a higher level of barrier penetration could be observed after the initial 5 min period.

For a given barrier to be considered reliable, it needed to be able to resist penetration for the entire 30 min period on 10 samples tested in parallel. The PS ink could only produce reliable barriers on Whatman 4 filter paper, and only with a drop spacing of 10 or 15 μm. With a 15 μm drop spacing, reliable barriers could be produced by printing barriers with a nominal width of 400 μm, resulting in actual barriers with a measured width of 883 ± 91 μm, while for 10 μm drop spacing, a nominal barrier 300 μm wide was required resulting in a measured barrier width of 996 ± 114 μm. Examples of printed barrier patterns after testing are shown in Figure 5, where cyan dyed channels indicate ones where coloured water wicked past the barrier while magenta dyed channels indicate ones where the barrier was not penetrated.

When PS ink was used with a drop spacing of 20 μm or more, or with Whatman 1 filter paper, full depth coverage could no longer be achieved. Instead, the reverse side of the printed patterns remained partially hydrophilic, allowing liquid to leak past. This is easily observable on the reverse side of the samples, as shown in Figure 6, where the liquid, having penetrated the initial barrier is not fully contained by the channel beyond but starts to spread further. This difference in depth coverage is not due to the thickness of the sheet, since Whatman 1 is actually slightly thinner than Whatman 4.

AKD and AKD-PS inks could produce reliable barriers on both Whatman 1 and Whatman 4 filter papers with all tested drop spacing values (up to 50 μm). The measured widths for the narrowest reliable barriers for these inks with different print settings are shown in Figure 7. Required nominal line widths for these barriers ranged from 50 to 450 μm, increasing as drop spacing increased. Notice, that for a number of these samples printed with close drop spacing, line spreading of the channel walls constricted the channel beyond the barrier so much that measuring the actual barrier width reliably was no longer possible.

As can be seen from Figure 7, there are no clear relationships between barrier width and drop spacing, paper type or ink type. Reliable barriers could be produced with a variety of settings for these inks as long as the nominal line width would be set large enough to ensure that a continuous barrier was formed on the reverse side.

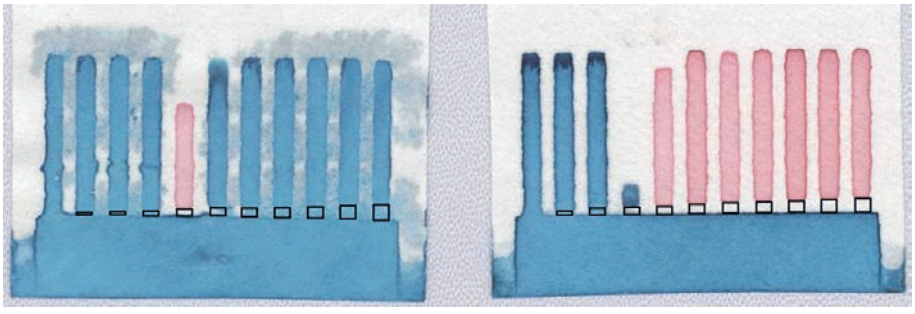

Figure 5: Examples of barrier tests, printed with PS ink at drop spacing of 15 μm on Whatman 1 (left) and Whatman 4 (right) filter papers; for clarity, printed barriers have been outlined with rectangles

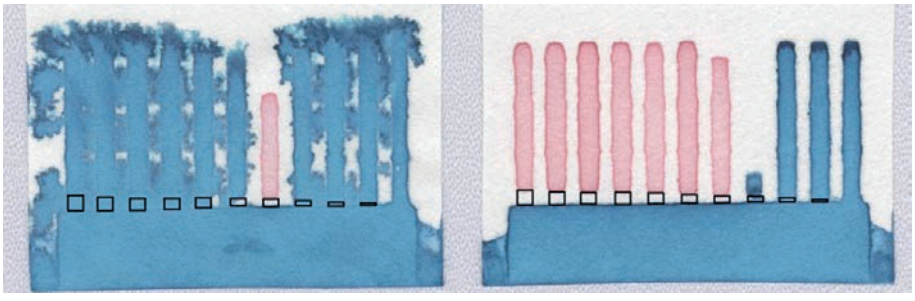

Figure 6: Reverse side views of the samples shown in Figure 5; on Whatman 1 (left), significant liquid spreading on the reverse side can be observed; barriers have been outlined with rectangles, as in Figure 5

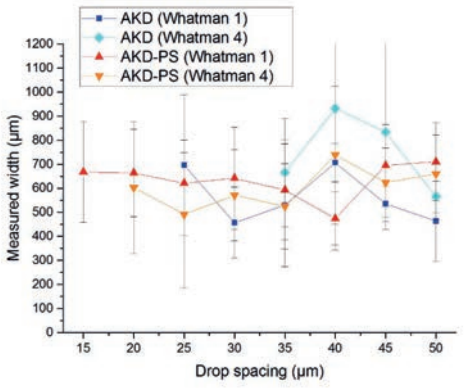

Figure 7: Measured widths of reliable barriers printed with AKD and AKD-PS inks

3.4 Hydrophilic channels

For producing narrow, fast wicking channels, the PS ink performed well. Using Whatman 4 filter paper and 15 µm drop spacing, channels down to a measured width of 680 ± 80 µm on the printed side could be produced, with dyed water consistently wicking a 30 mm distance along a channel within 5 minutes on all 10 samples. The nominal width of these channels was 1 300 µm, with the difference being due to line spreading of the surrounding barriers.

With AKD and AKD-PS inks, no fast-wicking channels could be produced. Rather, the water in the channels travelled so slowly that it could not even reach the top of the channel when the observation time was extended to 10 minutes. Close observation of these channels during tests indicated that the liquid front did not travel the whole width of the channel, unlike with channels printed with PS ink. Instead, the liquid wicked initially along the middle of the channel and then spread slowly to the sides of the channel. Even on the post dried sample, as shown in Figure 8, the wedge-shaped wicking front can be observed. The wider the channel, the longer the wicking front would advance within the given time.

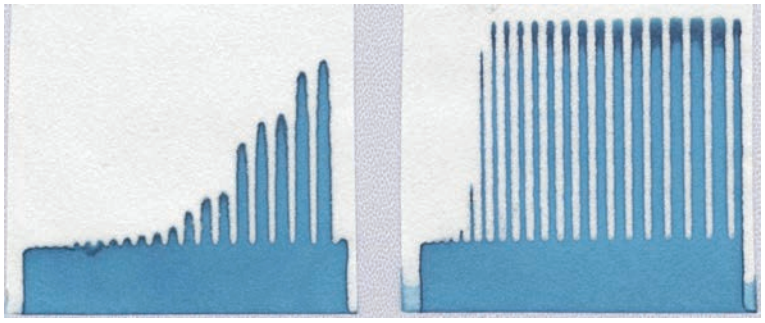

Figure 8. Examples of channel tests, printed on Whatman 4 filter paper with AKD ink at a drop spacing of 45 µm (left) and with PS ink at a drop spacing of 15 µm (right)

4. Discussion

4.1 Ink and substrate properties

In the light of the observations made in the previous section, the following commentary on correlations between the applied parameters of the inks, printing and substrates is offered.

All three inks could be jetted successfully. However, plain AKD ink featured limited jetting performance, being restricted to 2 kHz jetting and displaying velocity peaking. This is likely due to the low viscosity of the AKD ink, being very close to that of pure solvent. Adding a small amount of PS as a rheological modifier to produce AKD-PS ink resulted in a slight positive increase in low shear viscosity and, consequently, a significant improvement in jettability. This viscosity-related improvement in jettability might be partially due to a resulting viscoelastic behaviour leading to a temporary elastic response while under high stress in the print head. While strongly viscoelastic behaviour, such as exhibited by solutions containing high molecular weight polymers, can limit jettability (de Gans et al., 2004), a low level of viscoelasticity might actually improve jettability of otherwise low viscosity solutions. However, in this study the actual viscoelasticity of the inks was not measured.

The PS ink could achieve reliable full depth penetration on Whatman 4 filter paper, but not on Whatman 1, indicating that there is a significant substrate property difference between these two papers. It cannot be due to thickness, as Whatman 4 is actually the thicker of the two. Both papers are also reported to contain fibres of effectively the same dimension (Evans et al., 2014). Whatman 4, however, has significantly higher air permeability, which could suggest a correlation, though as gas and liquid may travel in quite different fashions through a substrate, this might not apply to all substrates.

Nevertheless, the path travelled by liquid through the sheet was presumably more tortuous in Whatman 1.

The AKD ink proved to be superior in depth penetration. This is at least partly due to the lower viscosity of the AKD ink, not only when jetted initially on paper, but also during the spreading and drying period when liquid viscosity increases due to solvent evaporation. However, the penetration might be further aided by the curing step, where the AKD is heated well above its melting point of ca. 50 ºC, providing it with an opportunity to spread slightly further than where it was initially deposited during drying. Adding some PS to AKD ink did not have any significant effect on this spreading behaviour.

The PS ink produced patterns with sharply defined edges, suggesting that there was a sufficient amount of PS on the edges of the printed patterns to produce clear contrast between the untreated and hydrophobised regions. Actually, there was some indication that the PS concentrations might actually be slightly higher at the edges of the printed patterns, which could be a result from the "coffee stain" phenomenon, where dry solids contained within a drying drop are deposited at the edges, most likely by Marangoni flow. However, this would require further characterisation before it could be confirmed.

On the other hand, with AKD and AKD-PS inks the edge regions were poorly defined, containing a semi-hydrophobised border area where water could advance slowly. This border area resulted in slowly wicking channels, as the central part of the channel also needed to feed these areas on the sides. This poor edge definition could be caused by affinity between AKD and fibre surfaces, leading to partial separation of AKD from the ink as it spreads, and resulting in only small amounts of AKD being deposited at the edges. Again, further studies would need to be performed to characterise this behaviour more fully.

4.2 Ink volume versus pore volume

Information provided by the line spreading tests can be used to calculate the effectively hydrophobised pore volume, V_{hpores}, for a section of a hydrophobic barrier. In parallel, the actual ink volume, V_{ink}, consumed to print the same section can be calculated from the print settings. For the following analysis, we choose this barrier section to consist of a single transverse line of printed drops.

We can consider this transverse line across a barrier to consist of a number of printed dots, N, defined by the drop spacing distance, d, and the nominal print setting width of the barrier, w_{n}, and given by Equation 4.

$$N = w_{\mathrm{n}} / d \qquad [4]$$

The N drops, therefore, deliver the volume of ink, V_{ink}, across the barrier width (Equation 5),

$$V_{\mathrm{ink}} = NV_{\mathrm{drop}} \qquad [5]$$

where V_{drop} is the volume of ink jetted in a single drop.

As an aside, we can also determine the available pore volume V_{pores} that is present underneath this line of drops, assuming perfect merging of the drops on the surface (Equation 6),

$$V_{\mathrm{pores}} = Nd^2h\varepsilon \qquad [6]$$

where, as before, d is the drop spacing, N the number of drops, h the substrate thickness and ε its fractional porosity. This available pore volume is, however, not necessarily saturated with ink, depending on the flow properties of the ink inside the substrate structure, and so we need to consider the realistic situation of diminishing contacted volume as the ink penetrates.

If we assume that the penetration of the ink reaches the complete thickness, as required for a satisfactory barrier, and that the cross-sectional penetrated profile is, in a first approximation, that of a wedge, as shown schematically in Figure 9, we may determine the effectively hydrophobised pore volume V_{hpores} underneath the printed transverse line by Equation 7,

$$V_{\mathrm{hpores}} = d\left(\frac{w_{\mathrm{p}} + w_{\mathrm{r}}}{2}\right)h\varepsilon \qquad [7]$$

defining w_{p} as the transverse line length (width) of the barrier on the printed side and w_{r} the observed barrier width on the reverse side, created by penetration.

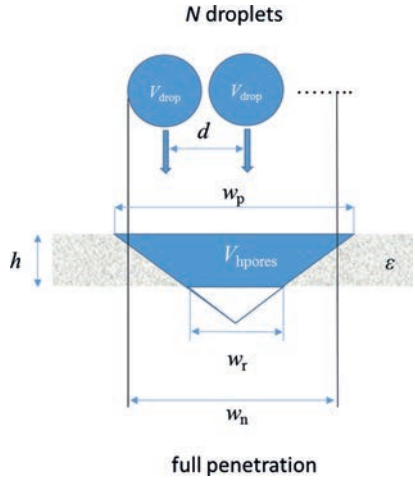

Figure 9: Schematic showing the applied drop volume V_{drop} with a drop spacing d, which is applied to the substrate of thickness h to form a nominal transverse barrier width w_n having a wedge-shaped cross-section of width w_p and w_r on the printed and reverse sides, respectively, such that the pore volume affected by the hydrophobising agent is V_{hpores}

The ratio V_{hpores}/V_{ink} informs us about the mechanism of ink distribution and its hydrophobising impact (Equation 8),

$$\frac{V_{hpores}}{V_{ink}} = \frac{V_{hpores}}{NV_{drop}} = \frac{d\left(\frac{w_p + w_r}{2}\right)h\varepsilon}{\left(\frac{w_n}{d}\right)V_{drop}} = \frac{d^2 h\varepsilon (w_p + w_r)}{2w_n V_{drop}} \quad [8]$$

such that, when the volume of hydrophobised pores exceeds that of the applied volume of ink, $V_{hpores}/V_{ink} > 1$, we can assume that ink has penetrated, at least at the latter stages, by film flow without filling the total available pore volume.

Assuming that the drop volume V_{drop} is the nominal 10 pl and using substrate properties given in Table 1, V_{hpores}/V_{ink} values can be calculated for the lines printed in the present study. They are presented in Figure 10 for Whatman 4 filter paper. For Whatman 1, the calculated V_{hpores}/V_{ink} ratios are around 14 % lower.

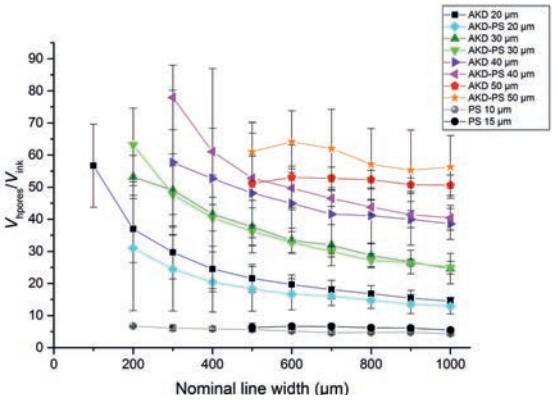

Figure 10. V_{hpores}/V_{ink} ratios for lines printed on Whatman 4 filter paper, as a function of nominal line width for a range of inks and drop spacing values

The values of V_{hpores}/V_{ink} vary quite a bit, from around 5 for PS ink to over 50 for AKD containing inks printed with large drop spacing. They are all significantly higher than 1, indicating that the hydrophobising ink does not completely fill the pore volume available beneath the applied ink. This confirms the suggestion that the ink spreading has primarily taken place through film flow on fibre surfaces, rather than through complete filling of the pores. Previously, the initial advance of the water front on un-sized paper has been demonstrated to be similarly controlled by the surface film flow (Roberts et al., 2003).

Also the pore filling level was studied separately by inkjet printing wax, heated to make it melt and penetrate the full depth of the filter paper, and considering the weight of the deposited wax into the substrate layer in relation to the mass that could have been filled into the total available pore volume. Hydrophobic barriers covering the full depth of the paper can be produced by a wax application that fills only 19 % of the paper pore volume (Wang et al., 2014). While not explicitly stated by the authors, these results indicate that melted wax must have spread primarily by surface film flow rather than by bulk flow within a saturated pore volume.

4.3 Comparison with previous studies

In a previous study, featuring PS as printed hydrophobising material, Olkkonen, Lehtinen and Erho (2011) tested chromatography paper (Whatman grade 1 Chr, thickness 180 µm, basis weight unspecified) and found that it could not be hydrophobised to a sufficient depth by applying a single flexographic printing on one side. Rather, each side needed to be printed, one side with the actual pattern and the reverse side with 100 % coverage. However, in the current study, PS could be successfully used to produce barriers with a single printing, provided that the substrate allows the ink to penetrate rapidly. This difference in performance may be attributed to both a higher volume of ink transferred by inkjet compared to flexography and to differences in ink viscosity due to ink composition. While both studies used xylene-based ink with 5 % by weight PS content, the current study uses PS with a lower molecular weight (35 kDa vs. 290 kDa) to aid mobility further, resulting in a significant difference in viscosity (1.2 vs. 6 mPa·s). Perhaps improved penetration depth using flexography could be achieved by using a lower viscosity PS solution as the ink. However, it is also possible that the demonstrated difference in performance might be due partially to the different substrates used.

AKD containing inks displayed poor edge definition of printed patterns, a property not reported in a previous study featuring AKD based ink printed on Whatman 4 filter paper (Li, Tian and Shen, 2010). This prior report used n-heptane as the solvent, which has higher vapour pressure and lower surface tension than p-xylene, resulting in reduced spreading on the substrate before drying. This may have resulted in less noticeable unevenness at the edges. The difference cannot have been due to substrate properties, since identical substrates were used in both studies.

The barrier and channel dimensions reported in this study for inkjet printed PS ink are in the same region as those previously reported for other printing methods and materials. The channel width of 680 ± 80 µm, as reported in the present study, matches the 700 µm channel width reported for inkjet printed PDMS on Whatman 1 filter paper (Määttänen et al., 2011), while being slightly wider than the 500 µm width reported for flexographically printed PS (Olkkonen, Lehtinen and Erho, 2011) and the 561 ± 45 µm width reported for inkjet printed hot-melt wax (Carrilho, Martinez and Whitesides, 2009). Similarly, the barrier width of

883 ± 91 μm is quite close to the 850 ± 50 μm width reported for inkjet printed hot-melt wax. Two-sided flexographic printing with PS ink could achieve narrower 400 μm wide barriers.

Perhaps resolution in the present study could have been improved by trying two sided printing, with the reverse side printed using 100 % coverage, but with a sufficiently sparse drop spacing of 20–25 μm to ensure that the ink printed on the reverse side does not penetrate the full depth of the substrate. This would result in the ink printed on the primary side having to penetrate to a lesser depth in order to produce reliable barriers. Thus narrower lines, penetrating less in depth but resulting in narrower barriers, could be printed.

5. Conclusions

PS containing solutions can be inkjet printed to provide well-defined hydrophobic patterning on porous substrates. However, the application window for the studied PS ink was rather narrow, requiring a suitable substrate for the PS ink to allow it to penetrate the full depth of the substrate.

The AKD ink was found to provide superior penetration and hydrophobising properties when compared to PS, although it suffered from limited jetting performance. The latter could be improved by adding some PS to the ink as a rheological modifier. However, patterns printed with AKD containing inks featured poor edge definition, not reported in previous studies.

Comparison of hydrophobised substrate pore volumes and printed ink volumes revealed that the printed ink volume could have filled only a small portion of the covered pore volume. This indicates that the ink spread primarily through film surface flow along fibre surfaces, rather than by complete filling of pores. It is expected that the inkjet technique and inks developed here could be further enhanced by better definition of the substrate structure, which is a topic for future work.

Acknowledgements

The alkyl ketene dimer sample used in this study was donated by Chemigate Oy. Funding for the project was provided by Omya International AG.

References

A-Alamry, K., Nixon, K., Hindley, R., Odel, J.A. and Yeates, S.G., 2011. Flow-induced polymer degradation during ink-jet printing. *Macromolecular Rapid Communications*, 32(3), pp. 316–320.

Abe, K., Suzuki, K. and Citterio, D., 2008. Inkjet-printed microfluidic multianalyte chemical sensing paper. *Analytical Chemistry*, 80(18), pp. 6928–6934.

Apilux, A., Ukita, Y., Chikae, M., Chailapakul, O. and Takamura, Y., 2013. Development of automated paper-based devices for sequential multistep sandwich enzyme-linked immunosorbent assays using inkjet printing. *Lab on a Chip*, 13(1), pp. 126–135.

Ballerini, D.R., Li, X. and Shen, W., 2012. Patterned paper and alternative materials as substrates for low-cost microfluidic diagnostics. *Microfluidics and Nanofluidics,* 13(5), pp. 769–787.

Carrilho, E., Martinez, A.W. and Whitesides, G.M., 2009. Understanding wax printing: A simple micro-patterning process for paper-based microfluidics. *Analytical Chemistry*, 81(16), pp. 7091–7096.

de Gans, B., Kazancioglu, E., Meyer, W. and Schubert, U.S., 2004. Ink-jet printing polymers and polymer libraries using micropipettes. *Macromolecular Rapid Communications*, 25(1), pp. 292–296.

Dharmaraja, S., Lafleur, L., Byrnes, S., Kauffman, P., Buser, J., Toley, B., Fu, E., Yager, P. and Luatz, B., 2013, Programming paper networks for point of care diagnostics. In: SPIE *Microfluidics, BioMEMS, and Medical Microsystems XI*. San Fransisco, February 2, 2013. International Society for Optics and Photonics.

Dungchai, W., Chailapakul, O. and Henry C.S., 2011. A low-cost, simple and rapid fabrication method for paper-based microfluidics using wax screen-printing. *Analyst*, 136(1), pp. 77–82.

Evans, E., Gabriel, E.F.M., Coltro, W.K.T. and Garcia, C.D., 2014. Rational selection of substrates to improve color intensity and uniformity on microfluidic paper-based analytical devices. *Analyst*, 139(9), pp. 2127–2132.

Hoath, S.D., Hutchings, I.M. and Martin, G.D., 2009. Links between ink rheology, drop-on-demand jet formation, and printability. *Journal of Imaging Science and Technology*, 53(4), 041208.

Hoath, S.D., Hsiao, W., Jung, S., Martin, G.D., Hutchings, I.M., Morrison, N.F. and Harlen, O.G., 2013. Drop speeds from drop-on-demand ink-jet print heads. *Journal of Imaging Science and Technology*, 57(1), 10503.

Jang, D., Kim, D. and Moon, J., 2009. Influence of physical properties on ink-jet printability. *Langmuir*, 25(5), pp. 2629–2635.

Jung, S., Hoath, S.D. and Hutchings, I.M., 2013. The role of viscoelasticity in drop impact and spreading for inkjet printing of polymer solution on a wettable surface. *Microfluidics and Nanofluidics*, 14(1-2), pp. 163–169.

Koivula, H., Pelton, R., Brennan, J.D., Grenon, J. and Manfred, T., 2013. Flexographic printability of sol-gel precursor dispersions for bioactive paper. *Nordic Pulp & Paper Research Journal*, 28(3), pp. 450–457.

Koivunen, R., 2014. *Inkjet-printed hydrophobic patterning of porous substrates for microfluidic applications*. MSc. Aalto University.

Li, X., Tian, J., Nguyen T. and Shen, W., 2008. Paper-based microfluidic devices by plasma treatment. *Analytical Chemistry*, 80(23), pp. 9131–9134.

Li, X., Tian, J. and Shen, W., 2010. Progress in patterned paper sizing for fabrication of paper-based microfluidic sensors. *Cellulose*, 17(3), pp. 649–659.

Liana, D.D., Raguse, B., Gooding, J.J. and Chow, E., 2012. Recent advances in paper-based sensors. *Sensors*, 12(9), pp. 11505–11526.

Määttänen, A., Fors, D., Wang, S., Valtakari, D., Ihalainen, P. and Peltonen, J., 2011. Paper-based planar reaction arrays for printed diagnostics. *Sensors and Actuators B: Chemical*, 160(1), pp. 1404–1412.

Martinez, A.W., Butte, M.J., Whitesides, G.M. and Phillips, S.T., 2007. Patterned paper as platform for inexpensive, low-volume, portable bioassays. *Angewandte Chemie (International ed.)*, 46(8), pp. 1318–1320.

Martinez, A.W., Phillips, S.T. and Whitesides, G.M., 2008. Three dimensional microfluidic devices fabricated in layered paper and tape. In: *Proceedings of the National Academy of Sciences of the United States of America*, 105(50), pp. 19606–19611.

Maejima, K., Tomikawa, S., Suzuki, K. and Citterio, D., 2013. Inkjet printing: an integrated and green chemical approach to microfluidic paper-based analytical devices. *RSC Advances*, 3(24), pp. 9258–9263.

Olkkonen, J., Lehtinen, K. and Erho, T., 2011. flexographically printed fluidic structures in paper. *Analytical Chemistry*, 82(24), pp. 10246–10250.

Roberts, R.J., Senden, T.J., Knackstedt, M.A. and Lyne, M.B., 2003. Spreading of aqueous liquids in unsized papers is by film flow. *Journal of Pulp and Paper Science*, 29(4), pp. 123–131.

Wang, J., Monton, M.R.N, Zhang, X., Filipe, C.D.M., Pelton, R. and Brennan, J.D., 2014. Hydrophobic sol-gel channel patterning strategies for paper-based microfluidics. *Lab on a Chip*, 14(4), pp. 691–695.

Xu, Y. and Enomae, T., 2014. Paper substrate modification for rapid capillary flow in microfluidic paper-based analytical devices. *RSC Advances*, 4(25), pp. 12867–12872.